IEEE Access
Multidisciplinary | Rapid Review | Open Access Journal

Received January 19, 2017, accepted February 10, 2017, date of current version April 24, 2017.

Digital Object Identifier 10.1109/ACCESS.2017.2674019

Plasma and Fields Evaluation at the Chinese Seismo-Electromagnetic Satellite for Electric Field Detector Measurements

PIERO DIEGO[1], IGOR BERTELLO[1], MAURIZIO CANDIDI[1], ALESSANDRO MURA[1], GIULIANO VANNARONI[1], AND DAVIDE BADONI[2]

[1]INAF/IAPS, 00133 Rome, Italy
[2]INFN Section Rome 2, 00133 Rome, Italy

Corresponding author: P. Diego (piero.diego@iaps.inaf.it)

This work was supported by the Italian Space Agency in the frame of the Progetto Premiale Limadou phase B/C/D1 under Grant CUP F84G14000080005.

ABSTRACT Model predictions are presented to evaluate the electrodynamic parameters as expected at the orbit of the China Seismic-Electromagnetic Satellite (CSES). The main objective of this paper is that of improving the accuracy of the electric field detectors (EFDs), which are installed on CSES and will measure the field vector in a wideband from dc up to 3.5 MHz. The electric field components are derived from the probe floating potential readings, thus an accurate characterization of the space environment is needed to model the currents collected from the ionosphere and establish the EFD probe response. The plasma environment and the magnetic field along the orbit are determined using the standard IRI and IGRF models. Simulations are used to determine the bias currents, which have to be applied to the probes to minimize the contact impedance between the EFDs and the ionospheric plasma. Correction voltages required to remove the $\vec{v} \times \vec{B}$ electric field from the EFD measurements are also estimated.

INDEX TERMS Electric potential, ionosphere, magnetic fields, plasma sheaths, probes.

I. INTRODUCTION

The China Seismic-Electromagnetic Satellite (CSES) has the main objective of monitoring possible Earthquake related electromagnetic emission in the ionosphere. The CSES mission will study ionospheric perturbations that may be associated with earthquakes, and plans to explore new approaches for short term forecast, as well as a new perspective for theoretical studies of the mechanism of earthquake preparation processes. The program will test the reliability and effectiveness of the proposed electromagnetic satellite monitoring system by utilizing a set of new techniques and equipment, in order to obtain world-wide data on the space environment with respect to electromagnetic fields, plasma and precipitation of energetic particles [1], [2]. The CSES science objectives are detailed in [3]. CSES is a 3-axis attitude stabilized platform and will be placed in a Sun-synchronous circular orbit at an altitude of about 500 km, with descending node at 14:00 LT [4] (launch is currently planned for mid 2017).

The purpose of this paper is the description of procedures to retrieve the ionospheric electric field components from data analysis of the EFD instrument; this is the payload on board CSES devoted to the measurement of the ambient electric field. The EFD payload has been conceived with objectives and specifications very similar to the ICE experiment (Instrument Champ Electrique), already flown on board the DEMETER satellite [1]. It consists of four floating probes located at the tips of four booms (about 4 meters long) deployed from the spacecraft. The field is measured from the potential differences between different pairs of sensors to determine the component of the electric field along the direction defined by the probe pair location. The configuration of the booms deployed from CSES is shown in Fig.1. Note that CSES is attitude stabilized and that the four sensors are deployed in directions which fall neither in the wake region of the satellite body nor in the wake of the other booms. This makes sure that electric field measurements are not perturbed by the electrostatic wakes usually observed on similar instruments installed on board spinning platforms [5]. The electric field components are determined in the non-orthogonal boom system, and then transformed to a more suitable orthogonal reference frame which uses Radial, Along-track and Cross-track components. The Radial component is parallel to the

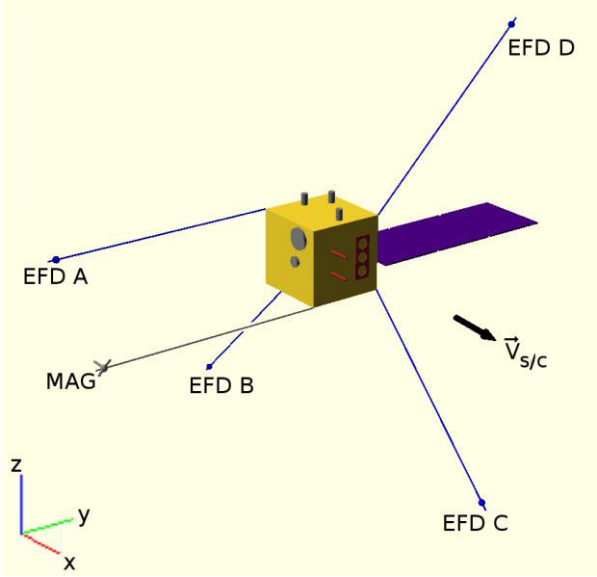

FIGURE 1. Schematic diagram of CSES satellite indicating the deployed boom geometry with respect to the orbital motion.

direction pointing to Nadir, the Along-track component is parallel to the satellite velocity vector and the Cross-track component is transverse and completes the orthogonal right handed frame.

Each probe consists essentially of a spherical electrode (6 cm diameter) equipped with embedded electronics including a unity gain amplifier (with a very high input impedance) and a current source which is capable of injecting the same prescribed level of bias current to each electrode to control its floating potential. The four probes are not swept in voltage during flight, but are designed to measure their floating potential in the plasma in a wide frequency band (from DC to about 3.5 MHz). The probes are also provided with cylindrical conducting stubs, bootstrapped at the potential of the electrodes; these are specifically designed to minimize the local potential perturbations produced by the presence of the conductive booms (electrically connected to the satellite ground). These features allow a high accuracy estimation of the AC and DC ionospheric electric field vector.

The accuracy of the electric field measurements relies on the capability of the sensors to precisely follow the local plasma potential fluctuations. Such measurements are mainly affected by the presence of a plasma sheath formed next to the electrode surface. The plasma sheath introduces, in series to the reading electrical circuit, a probe/plasma coupling impedance ($Z_c = R_{pl}//X_{Cpl}$) which should be maintained as small as possible compared with the preamplifier input impedance ($R_i \geq 10$ GΩ and $C_i \cong 10$ pF). Such a prescription reduces the relevant voltage divider attenuation and widens the amplifier high frequency response. The probe/plasma sheath impedance varies along the orbit as a function of the plasma parameters which, in turn, depend on the satellite position in space. In addition, the contact impedance depends on the electrode voltage w.r.t. the local plasma and exhibits its minimum value when the probe is biased at the plasma potential (V_{pl}). As discussed in detail in the following sections, the probe potential can be efficiently controlled by injecting a bias current to the electrode; consequently, the contact impedance can be minimized through an appropriate selection of such current. An important objective of this paper is to provide an outlook of the bias currents needed along the orbits of CSES which have been simulated considering that the mission will take place in the descending phase of the current solar cycle. As we will see later, a bias current in the range 5 μA $-$ 10 μA implies a plasma sheath resistance (R_{pl}) of the order of $10^4\Omega$, which minimizes at best the voltage divider effects at the typical CSES orbits examined in our simulations.

Another important element, which alters the probe potential measurements (and consequently the retrieved electric field), is the induced $\vec{v} \times \vec{B}$ field, where $\vec{v}$ is the orbital velocity and $\vec{B}$ the terrestrial magnetic field. The induced field produces a voltage along the wirings that electrically connect the various probes from the tips of the booms to the reading electronics box, located in the satellite interior. Such voltages are different for the various booms and are algebraically added to the potential actually sensed by each probe. Thus the induced voltages, relevant to the various probes, should be subtracted from data measured at the reading electronics box, to evaluate the ambient electric field.

II. PLASMA PARAMETERS AT CSES

The ionospheric plasma parameters depend on solar external forcing; plasma electron temperature and density change if exposed to different solar UV irradiance along the satellite orbits. Plasma density is the parameter which varies more drastically with latitude, showing at the dayside equator an increase of up to 10 times over what observed at polar latitudes; instead, on the nightside, only a moderate increase at low latitude (about 2 times higher near the equator) is observed.

Electron density and temperature have been retrieved from the International Reference Ionosphere (IRI) – 2007 model [6], available at: http://omniweb.gsfc.nasa.gov/vitmo/iri_vitmo.html

The IRI model was used for the whole solar cycle n. 23 (1996 – 2009) and, in particular, for the portion of descending phase of the cycle (2004 – 2005) which roughly corresponds (about 11 years later) to that in which CSES will start operation (2017).

The dataset retrieved from IRI shows an expected variability, at the CSES orbit, in the following ranges:

Plasma density: $7{\cdot}10^9 - 2{\cdot}10^{12}$ m^{-3}; Electron temperature: 1030 – 3289 K.

In order to concisely represent the solar cycle effect on the variability of these parameters, latitude averaged quantities and time averaged values have been calculated for January 1st, for each year of the entire solar cycle n.23; the computation has instead been made quarterly for years

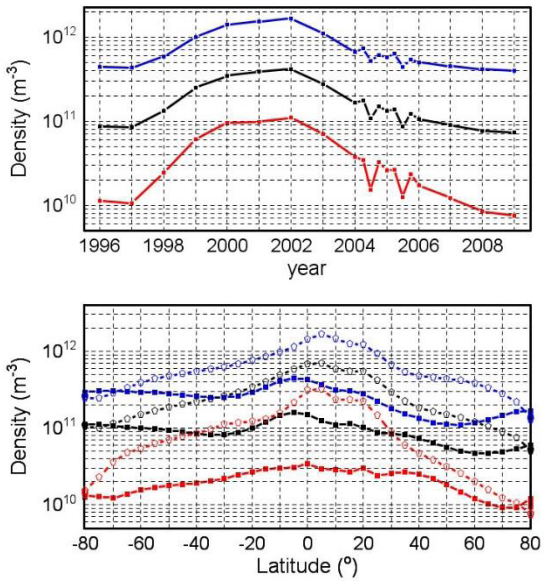

FIGURE 2. The top panel shows the maximum, average, and minimum values of electron densities modelled by IRI for solar cycle n.23 along an entire CSES orbit. The data refer to January 1st of each year; computations have been made quarterly in years 2004-2005 (January 1st, April 1st, July 1st, and October 1st). The plots marked with blue, black, and red symbols represent the maximum, average, and minimum values, respectively. In the bottom panel, the maximum, average, and minimum values, over an entire solar cycle, are represented as a function of the satellite latitude. Open markers refer to the dayside part of the orbits, while the solid symbols refer to the night side.

2004 and 2005, which are expected to be representative of the epoch during which CSES will be operational.

These values are shown in Figs. 2 and 3 along with the maxima and minima observed for the same orbits.

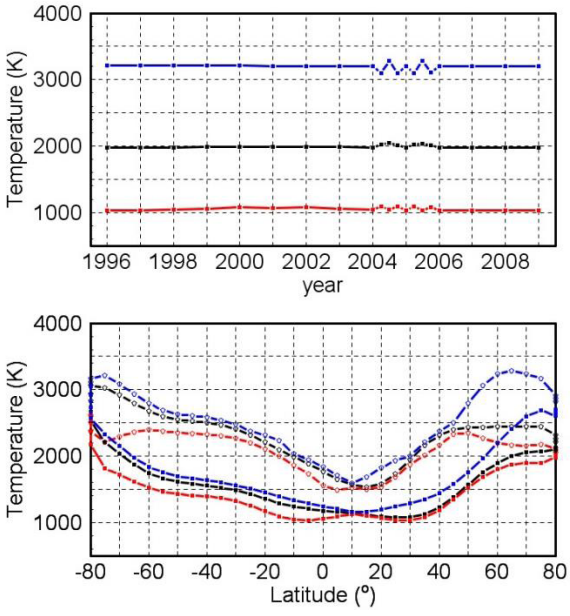

FIGURE 3. Same as Fig.2, referring to the plasma temperature.

The values in the sub-period 2004-2005 have been detailed with higher resolution (i.e. retrieved every 3 months from IRI), since this phase of the cycle may be more representative of the conditions encountered by the CSES satellite during its initial operation, requiring a better analysis of seasonal effects.

III. PLASMA/PROBE COUPLING PARAMETERS

The probes of the EFD payload behave essentially as floating electrodes embedded within the ionospheric plasma. A conducting body in contact with a plasma attains a potential (denoted as floating potential) which can be theoretically estimated by imposing that the net current collected by the probe surface is equal to zero. In the case of the EFD probes, four contributions are relevant: electron collection, ion collection, photoelectron emission, and the current injected to the probe by the embedded current bias source. The floating potential condition can be expressed as:

$$\sum_{k} I_k = 0 \quad k = 1, \ldots, 4 \tag{1}$$

where the index k indicates the various equations for collected or emitted current contributions listed above; the equations of the currents associated with the various processes will be detailed in the following sections. All these terms can be expressed by voltage dependent equations and, in general, the procedure required to calculate the floating potential implies the determination of the entire probe current-voltage characteristic. This is obtained considering the various currents, expressed as a function of potential, for both $V > V_{pl}$ and $V < V_{pl}$.

A qualitative representation of the current-voltage characteristic of an electrode in a plasma is shown in Fig. 4.

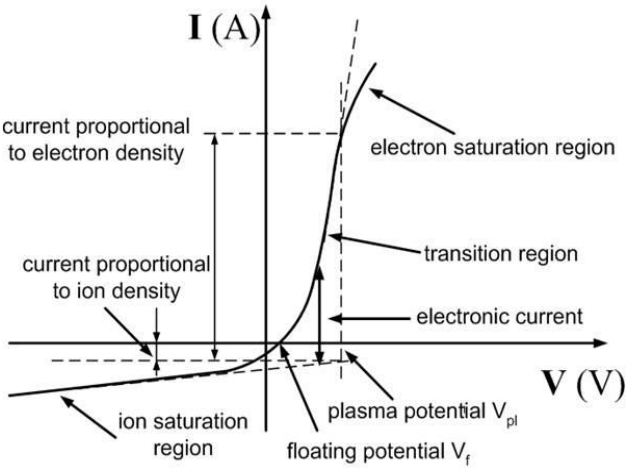

FIGURE 4. Current-voltage characteristic of a conducting electrode in a plasma.

Note that the embedded current generator is part of the EFD electronics and can be set by remote control during flight. This is used to modify the balance among the various currents, thus controlling the potential of the probe with respect to that of the local plasma. We remark however that, in flight, the EFD probes are not swept in voltage as usually performed on Langmuir probes to measure the

current-voltage characteristic, instead they float at a point of the curve which is close to the plasma potential. This is obtained by tuning the level of the bias current.

An important parameter, which needs to be computed at the various points along the characteristic curve, is the contact impedance ($Z_c = R_{pl}//X_{Cpl}$) between probe and plasma. The dynamical resistance R_{pl} at a point along the current-voltage curve (see Fig. 4) is defined as the reciprocal of the derivative of the current with respect to the potential, according to:

$$R_{pl}^{-1} = \left.\frac{dI_{tot}}{dV}\right|_{V=V_0} \tag{2}$$

where V_0 represents the potential value at which the dynamical resistance is determined. The contact resistance exhibits its minimum close to the plasma potential point (V_{pl}).

In the following, the expressions of the different currents listed above are given as a function of the probe voltage, and are used to determine the global characteristic of the electrode. Eq.1 is then used to estimate the new floating potential of the probe (V_f'), which is different from that of Fig. 4, since it is moved towards the plasma potential (V_{pl}) by the injection of the bias current. Finally Eq.2 is applied for the calculation of the relevant plasma coupling resistance (i.e. the $R_{pl}@V_f'$). Note however that the value computed through Eq.2 represents only an upper limit of Z_c, as a more complete analysis of the relevant equivalent circuit should include the capacitor C_{pl} associated to the plasma sheath which further reduces the impedance in particular at high frequency. Such a capacitance can be estimated by considering a spherical capacitor with the inner electrode having a radius equal to that of EFD probe separated by a Debye length from the outer electrode representing the unperturbed plasma [7]. The capacitance associated with such element is of the order of 10 pF, varying with the electron temperature and density between about 5 pF and 30 pF [8].

A. ELECTRON CURRENT COLLECTED FROM PLASMA AT $V < V_{pl}$ (RETARDING POTENTIAL)

In a plasma at thermal equilibrium, the velocities of the electrons are characterized by a Maxwellian distribution function, with thermal speed defined as:

$$v_{th} = \sqrt{\frac{8kT_e}{\pi m_e}}$$

where $k = 1.38 \cdot 10^{-23}$ J K^{-1}, $m_e = 9.1 \cdot 10^{-31}$kg.

For the electron temperatures expected in the ionosphere (1000-3000K) the electron thermal speed varies between $2 \cdot 10^5 - 3.4 \cdot 10^5$ m/s. In this case, the satellite velocity ($7.5 \cdot 10^3$ m/s) is much lower than the thermal speed, and can be neglected. The electron current collected by an electrode embedded in the plasma under a retarding potential (i.e. with $q(V\text{-}V_{pl}) < 0$) is given by [9], [10]:

$$I_e = \frac{1}{4} q n \sqrt{\frac{8kT_e}{\pi m_e}} S_e e^{\frac{q(V-V_{pl})}{kT_e}} \tag{3}$$

In Eq.3 n is the plasma density, S_e is the cross-section area of the probe for electron collection, V denotes the probe potential, and V_{pl} is the local plasma potential. If the gyroradius of electrons is larger (or of the same order of magnitude) than the probe radius, the electron speed is assumed to be isotropically distributed in space. This is the case applicable to the EFD probes, thus the cross-section S_e may be assumed equal to the area of the sphere $S_e = 4\pi R_p^2$.

As we can see from Eq.3 the electron current is proportional to the plasma density which, at the altitude of the CSES satellite, is expected to vary approximately between 10^{10} and 10^{12} m^{-3}. As an example, we can compute the current collected by the EFD probe (a sphere with radius of 3 cm), assuming average plasma parameters with electron temperature and density expected along the orbit equal to $T_e = 2000$ K and $n = 10^{11}$ m^{-3}, and assuming that the probe is biased at the plasma potential (i.e. at $V\text{-}V_{pl} = 0$). We obtain:

$$I_{e0} = \frac{1}{4} e n \sqrt{\frac{8kT_e}{\pi m_e}} 4\pi R_p^2 = 12.6\ \mu A.$$

The electron current collected at $V = V_{pl}$, is usually denoted as the random thermal current, and represents the current which would be collected by the probe under the effect of the electron temperature alone. Such a current is modulated by the exponential term in Eq.3 and strongly varies when the probe potential moves about the plasma potential. It is worth to notice that in the retarding electron collection regime the electron current collected by a probe is completely independent of the dimensions of the sheath [9].

B. ELECTRON CURRENT COLLECTED FROM PLASMA AT $V > V_{pl}$ (ACCELERATING POTENTIAL)

For accelerating potential, two possible conditions can be defined, depending on the relative dimension of the plasma sheath with respect to the probe radius. In particular, for plasma sheaths much thinner than the probe radius (thin sheath approximation) the collected current, for $V\text{-}V_{pl} > 0$, tends to flatten at a constant value approximately equal to the random thermal current. On the other hand, for plasma sheaths much thicker than the probe radius (thick sheath approximation), the collected current for $V\text{-}V_{pl} > 0$ tends to increase linearly vs. V, maintaining a constant slope equal to that exhibited by Eq.3 at the plasma potential (i.e. at $V = V_{pl}$) [9].

The thickness of the plasma sheath can be evaluated considering the Debye length λ_D as, at a first order of analysis, the sheath can be assumed to extend over several λ_D. The Debye length is:

$$\lambda_D = \left(\frac{kT_e \varepsilon_0}{nq^2}\right)^{1/2}. \tag{4}$$

As easily computed from Eq. 4, the Debye length, within the ionospheric ranges of electron temperature and density given above, can vary between about 0.2 cm and 4 cm.

Considering that, the true sheath dimension is equal to several λ_D lengths, we may assume that the minimum thickness could be of the order of 1 cm. Even assuming the minimum sheath dimension, the thin sheath condition $d_{sheath}/r_{probe} \ll 1$ is never rigorously satisfied, therefore the "thick sheath approximation" represents a regime which can reasonably be applied to the entire range of ionospheric conditions encountered by the EFD probes during the CSES mission. Such a choice is further motivated by the fact that a complete expression for determining the electron current under accelerating potential [9] in the transitional cases (i.e. between thin and thick sheath conditions) is hardly solvable, since an a priori knowledge of the sheath extent is needed, but not easily determined. The expression which describes the collected electron current I_e as a function of the electrode potential V (for $V > V_{pl}$) in the "thick sheath approximation" is [9], [10]:

$$I_e = \frac{1}{4} q n \sqrt{\frac{8kT_e}{\pi m_e}} S_e \left(1 + \frac{q\left(V - V_{pl}\right)}{kT_e}\right). \tag{5}$$

C. ION CURRENT COLLECTED FROM PLASMA (ACCELERATING POTENTIAL $V < V_{pl}$ AND RETARDING POTENTIAL $V > V_{pl}$)

Differently from the electrons, the ions, in the reference system moving with the satellite, are seen as a flux of particles coming from the ram direction with a velocity equal to that of the satellite (i.e. $v_i \approx 7.5\ 10^3$ m/s).

Therefore the space distribution of ion velocity implies that the probe cross section for ion collection is that of a flux tube, aligned with the satellite velocity vector, which for a spherical shape probe is $S_i = \pi R_p^2$. Thus the value of the ion current collected by the probe can be approximately estimated assuming a flux of mono-energetic ions with energy equal to:

$$K_{ion} = \frac{1}{2} m_i v_{orb}^2$$

Assuming an average mass unit of 20 (NO^+, O^+) [6] the resultant ion mass is $m_i = 3.3 \cdot 10^{-26}$kg with an associated kinetic energy of $K_{ion} = 9.4\ 10^{-19}$J (equivalent to $K_{ion/eV} = 5.9$ eV). The dominant ion species in the ionosphere at 500 km altitude is O^+ (mass unit 16), but variations may occur if electric fields are present. A model [11] shows that even moderate electric fields (of the order of 100mV/m) may induce chemical reactions and enhance the NO^+ ions concentration, making it comparable to the O^+ dominant species. With an average ion mass of 20 we have implicitly assumed a concentration ratio of about NO^+:O^+ = 1:8. Such assumption is not critical; in fact, we have verified that a change of the average ion mass (between 16 and 20) does not significantly modify the probe potential, as it is mainly controlled by the electron current through its sharp exponential term (see Fig. 4, and compare Eq.3 to the following Eq.6).

Given the positive charge of the ions, the accelerating potential condition is obtained for $V < V_{pl}$, whereas the retarding potential condition occurs when $V > V_{pl}$.

Using the same considerations already made for electron collection, we assume a thick sheath approximation for all the ionospheric conditions encountered along the CSES orbit, thus the ion current can be computed simply assuming the angular momentum conservation of particles [10]. The assumption of the thick sheath condition for ion collection is also reinforced by the analysis detailed in [12] which shows that, for negative probe polarizations the plasma sheath thickness is always significantly larger than the Debye length.

Then, the collected current (due to a mono-energetic beam of ions) can be expressed as:

$$I_i = \pi R_p^2 q n v_{orb} \cdot \left(1 - \frac{q\left(V - V_{pl}\right)}{K_{ion}}\right) \tag{6}$$

Note that, differently from the electron collection discussed in the previous section, this equation is valid for both retarding and accelerating potentials.

D. PHOTOELECTRON CURRENT

Photoelectron flux is emitted by the probe surface as an effect of the solar radiation. Typical values of the photoelectron current densities have been evaluated from theoretical modelling and in laboratory measurements; Table 1 quotes the photoelectron current densities (at 1 AU) of several conducting materials often used in the construction of probes [13]:

TABLE 1. Photoelectron current densities of several conducting materials.

Material	Current density J_{ph} ($\mu A/m^2$)
Al	42
Au	29
Stainless Steel	20
Vitreous Carbon	13
Graphite	4
Aquadag	18

Some data for the specific coating of the CSES EFD probes (i.e. the DAG 213 from Acheson) are reported in [14] and references therein, where a photoelectron current of 100nA is quoted for the EFW sensors of CLUSTER satellites. Given the dimensions of EFW probes (spheres of 8cm diameter) this corresponds to a photoemission current density of 20 μA/m^2, which, in turn, corresponds to the value used by the DEMETER investigators for the same coating of ICE probes [15].

The emitting surface for photoelectron current of a spherical probe with radius R_p under solar radiation is simply $S_{SR} = \pi R_p^2$; assuming a current density of $J_{ph} \cong 20\mu A/m^2$, the photoelectron current emitted by the EFD probe (6cm diameter) is:

$$I_{ph} = 20 \cdot 10^{-6} \pi R_p^2 = 0.057\ \mu A$$

Photoelectron emission may be assumed constant for $V \leq V_{pl}$ as the surface electric field favours the emission, and it is suppressed for $V > V_{pl}$. However, the latter assumption is only a crude approximation, as the emitted photoelectrons actually have a certain energy, sufficient to let them escape from the surface even at a moderate positive potential. Anyway the emission at positive potentials is completely masked by the strong current collection which, for $V > V_{pl}$, increases rapidly with V, above the random current which is already large. Indeed, such current, computed with the minimum values expected for electron temperature and density, is of about 0.8 μA (much larger than 0.057 μA). Therefore, we may neglect it and we may assume:

$$\begin{cases} I_{ph@V \leq V_{pl}} = 0.057\ \mu A \\ I_{ph@V > V_{pl}} = 0 \end{cases} \tag{7}$$

E. BIAS CURRENT

The current generator is used to modify the balance among the various currents, thus controlling the potential of the probe with respect to that of the local plasma. The probe potential is modified to drive it as close as possible to the local plasma potential, where the contact resistance exhibits the minimum value. Thus the capability of the probe to follow the fluctuations of the local plasma potential improves significantly. In the following section, the floating potential of the EFD probe is determined considering the various current terms and using the values of plasma density and electron temperature estimated with IRI along the CSES orbit. In addition, the plasma sheath contact resistance is calculated, in order to evaluate the more suitable bias current to be set during flight.

IV. FLOATING POTENTIAL AND PLASMA COUPLING RESISTANCE AS A FUNCTION OF n_{pl} AND I_{bias}

The total current collected by the EFD probe, at a prescribed voltage V, can be calculated by adding the contributions of the various equations given in Sect. 3.

In all equations a null local plasma potential (i.e. $V_{pl} = 0$) has been arbitrarily assumed; this assumption does not invalidate the results.

The expression derived from Eq. 1 is transcendent, and it can only be solved using a numerical approach. In particular we performed the calculation parametrically, by varying the potential between -10V and $+10$V with 10mV steps. The results shown in this paper have been obtained for positive bias currents of 0, 1, 5, and 10 μA (positive values only, see Fig. 2 in Pedersen *et al.* [16]). An example of results for a typical orbit is shown in Fig. 5, which is calculated with plasma data retrieved from IRI for January, 1st 2005, assumed to be roughly similar to the period when CSES will be launched (as already stated above).

The plasma coupling resistance is estimated from the inverse of the derivative of the collected current with respect to the potential, according to Eq.2. The resistance is computed by differentiating the algebraic sum of I_e and I_i equations (Eqs. 3, 5, and 6); contributions from I_{bias} and I_{ph} can be neglected, since they are constant terms. The analytical expression of the plasma coupling resistance plotted in the bottom panel of Fig. 5 is:

$$R_{pl}^{-1} = \left(qn\pi R_p^2\right) \cdot \left(\sqrt{\frac{8kT_e}{\pi m_e}} \cdot \frac{q}{kT_e} e^{\frac{q(V-V_{pl})}{kT_e}} + \frac{2q}{m_i v_{orb}}\right) \quad @V \leq V_{pl}$$

$$R_{pl}^{-1} = \left(qn\pi R_p^2\right) \cdot \left(\sqrt{\frac{8kT_e}{\pi m_e}} \cdot \frac{q}{kT_e} + \frac{2q}{m_i v_{orb}}\right) \quad @V > V_{pl} \tag{8}$$

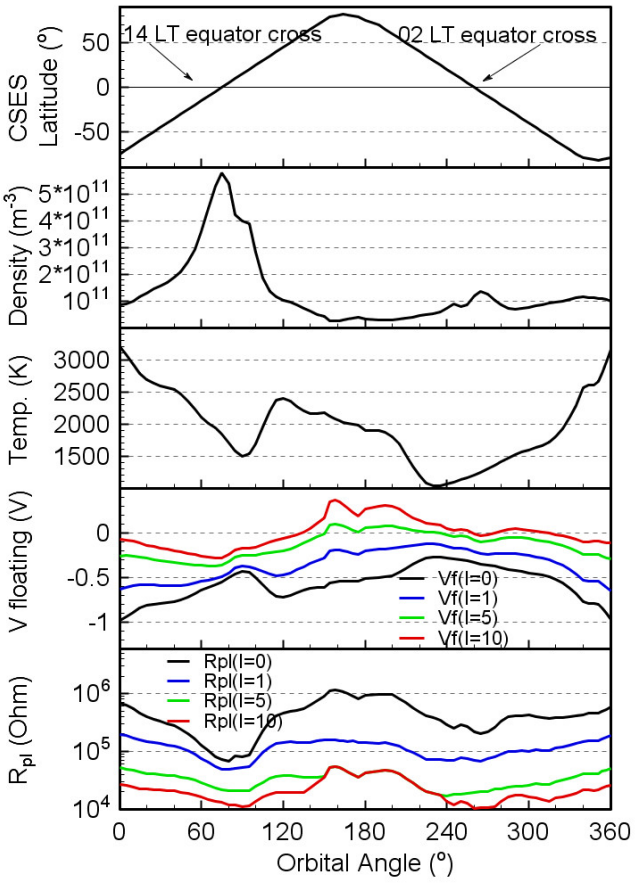

FIGURE 5. Plasma parameters, V_f, and Z_c computed for different bias currents. Data refer to January 1th, 2005. From top to bottom the various panels show: i) CSES latitude, ii) electron density, iii) electron temperature, iv) EFD floating potential and v) plasma sheath resistance; the values in panels iv) and v) are computed for the different bias currents (I_b = 0, 1, 5, and 10 μA) corresponding to the black, blue, green, and red curves respectively and for a fixed photoelectron current ($I_{ph} = 20\mu A/m^2$).

V. ANALYSIS OF PHOTO-ELECTRON CURRENT CONTRIBUTION

In order to quantitatively evaluate the contribution of photo electron current, which was assumed to be equal to zero in the previous analysis, we performed a parametric simulation to evaluate the effect on the floating potential fluctuations

and plasma sheath impedance. As discussed in the previous Sect. 3.4, the value of the photoelectron current of DAG-213 coating is not exactly known. In addition, it was experimentally observed that the emission of the current density J_{ph} is not at all a time stable process. In particular, during long operation in space, in several experiments a significant enhancement vs. time (by a factor up to 4) has been noted with respect to the values measured in the laboratory. Such behaviour has been correlated with possible ion implantation on the probe surface due to the ionospheric environment [16].

Moreover, a recent study [14] performed to evaluate the photoelectron yield from CLUSTER probes, showed that the DAG-213 coating may also be removed from the probe surface over time, due to interaction with the space environment. In such a case, after long exposure to plasma, the probes exhibited the photoemission properties typical of their substrate (Aluminium).

For this analysis we have selected the centre date of the studied period (that is January 1th, 2005) and we have recalculated V_f and R_{pl} for an intermediate bias current ($I_b = 5\mu A$) but for three different values of photoelectron current (even exceeding the values expected for DAG-213 and Aluminium in Tab. 1): $I_{ph} = 0\mu A$, $I_{ph} = 0.06\mu A$ ($J_{ph} = 20\mu A/m^2$), and $I_{ph} = 0.23\mu A$ ($J_{ph} = 80\mu A/m^2$).

No significant differences can be observed at the various photoelectron current levels, as shown in Fig. 6. The results show that V_f and R_{pl}, in the range of plasma parameters tested in our study for the CSES mission, are very weakly perturbed by the possible photoelectron current variations. Such a conclusion is also in agreement with the analysis on photoelectron current in a dense ionospheric plasma discussed in [16].

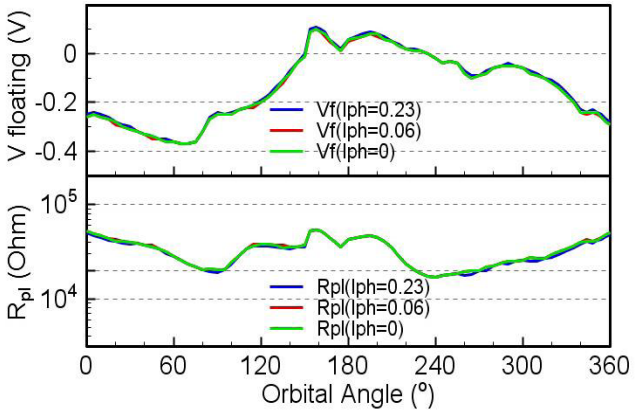

FIGURE 6. January 1st, 2005 values of V_f and R_{pl} computed at fixed $I_b = 5\mu A$ and different I_{ph} values. Green, red, and blue lines correspond to the three I_{ph} currents 0 μA, 0.06 μA, and 0.23 μA, respectively.

VI. TERRESTRIAL MAGNETIC FIELD EFFECTS AT CSES

The Earth magnetic field at CSES cannot be neglected when the detection of electromagnetic fields is attempted. The effect of the geomagnetic field is twofold:

i- The motion of CSES through the B magnetic field lines induces an electric field along conducting parts of the satellite body, according to the formula $\vec{E} = \vec{v} \times \vec{B}$, where $\vec{v}$ is the satellite velocity vector (about 7.5 km/s).

This electric field will induce a voltage drop among each pair of spheres, and between the probes and the satellite body; this may influence the potential of each of them w.r.t. the local plasma potential. This net electric field, and its time dependence along the orbit, will have to be considered when we attempt the measurement of both static and variable electric fields.

ii- The local value of the magnetic field represents a natural baseline w.r.t. which the variable part of the magnetic field will have to be determined.

The value of the Earth magnetic field is nowadays well known. A model of the Earth's magnetic field will be adopted and, at each point along the orbit, its value and orientation w.r.t. the satellite boom directions will be used to determine the motion induced electric field, so that it may be subtracted from the measurements, and the true ambient electric field can be measured. During the real mission data from the on board magnetometer will be used to determine the $\vec{E} = \vec{v} \times \vec{B}$; in this paper the data are simulated as described in the following section.

A. IGRF MODEL DATA AND MAGNETIC FIELD VARIABILITY ALONG CSES ORBIT

The International Geomagnetic Reference Field (IGRF) model is the empirical representation of the Earth's magnetic field recommended for scientific use by a special Working Group of the International Association of Geomagnetism and Aeronomy (IAGA). The IGRF model represents the main (core) field without external sources. The model employs the usual spherical harmonics expansion of the scalar potential in geocentric coordinates. The IGRF model coefficients are based on all available data sources including geomagnetic measurements from observatories, ship, aircraft and satellites.

The IGRF [17] is described in http://ccmc.gsfc.nasa.gov and can be retrieved at http://ccmc.gsfc.nasa.gov/modelweb/models/igrf_vitmo.php

An evaluation for year 2005 of the expected magnetic field along a nominal CSES orbit is shown in Fig. 7. The magnetic field components B_{North}, B_{East}, B_{Down}, the total B intensity and the induced electric field components vxB_{North}, vxB_{East} and vxB_{Down} are shown. We notice that, as expected since we are dealing with a modified dipole geometry, the maxima of the vertical component are attained at maximum latitude; such maxima also reflect in the maxima of the total field, since in a dipole geometry B increases with latitude. B_{North} instead maximizes at the equator. The deviations from simple dipole geometry reflect the distorted geometry of the actual Earth's magnetic field.

B. CORRECTION ALGORITHM FOR EFD ELECTRIC FIELD MEASUREMENT

Assuming a nominal orbit and satellite attitude, and given the satellite boom geometry, it is possible to infer the induced

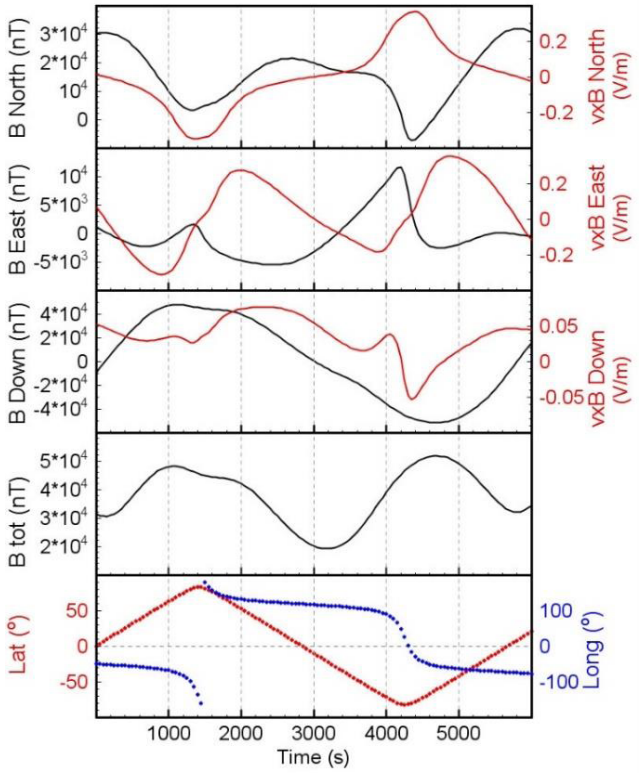

FIGURE 7. Predicted values of ambient magnetic field (black lines) and induced electric field (red lines) along a CSES nominal orbit (descending node at 14:00 L.T. and geographic longitude 120° for this specific orbit chosen). Red lines represent the values of the induced electric field components expressed in the IGRF reference frame. Satellite longitude and latitude are shown in the bottom panel.

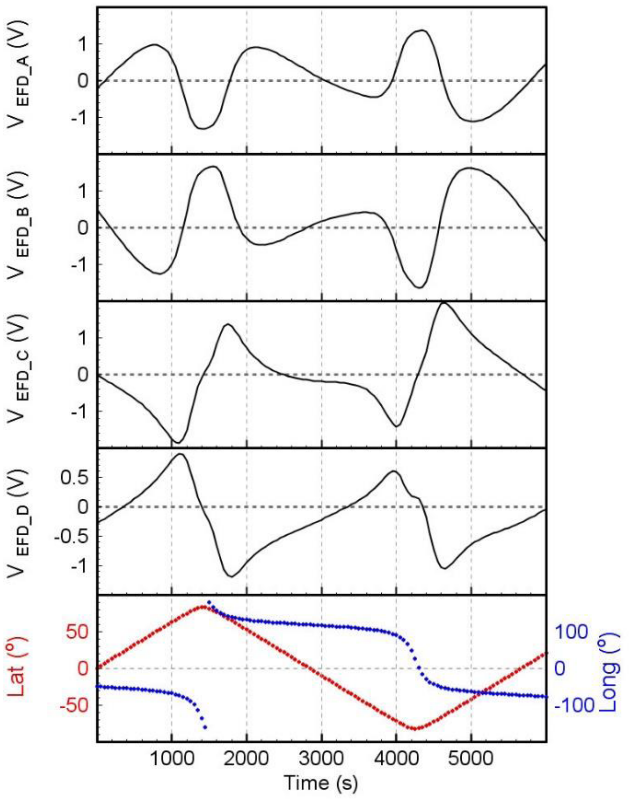

FIGURE 8. Voltages induced in the four cables connecting the EFD probes to the reading electronics box (assumed located at the satellite-rocket docking surface). Such values should be added to the actual voltages measured by electronics to provide corrected data.

electric field, across each pair of probes. This has been computed and is plotted in Fig. 7 (red lines).

The East-West component of the induced electric field has secondary minima at high latitudes, where the satellite velocity vector is across the ambient magnetic field, and a sizeable vertical component develops.

We notice that, in the ascending part of this particular orbit, the induced electric field components, both vertical and East-West, are minimum at the geomagnetic equator since there the field is horizontal and generally directed towards the magnetic pole, i.e. roughly parallel to the direction of CSES flight. Vertical components of the field develop as CSES moves away from the equator, and give rise to an East-West induced electric field. In the descending part of the orbit, the geometry of the flight direction w.r.t. the ambient magnetic field is different, and this reflects in the values of the $\vec{v} \times \vec{B}$ components.

Few additional words are necessary to explain the algorithm used to correct the readings of EFD probe potentials. The output voltages of the EFD probes are measured through high input impedance electronics contained in a box located in the satellite interior. The $\vec{v} \times \vec{B}$ electric field associated with the satellite motion induces a voltage in the electrical harness, which extends from the tips of booms (i.e. from probes) up to the reading electronics box. The induced voltage can be easily determined through:

$$\Delta V_i = \left(\vec{v} \times \vec{B}\right) \cdot \vec{l}_i \quad i = 1, 2, \ldots, 4 \tag{9}$$

where $\vec{l}_i$ are the vectors which define the end points of the harness which connect each probe to the electronics box. Such voltages are different from one probe to another since the positions of the four probes w.r.t. the box which contains the reading electronics are different. The induced voltages, which vary along the orbit due to the $\vec{v} \times \vec{B}$ modulation, will algebraically add to the potential measured at the sensor outputs and, therefore, should be subtracted to determine the right values of the probe potentials (which are measured with respect to the satellite reference ground). However, while the coordinates of the probes are already known as given in Table 2 w.r.t. the satellite-rocket docking surface [18], those of the electronics box are not yet defined. Thus in this paper, we will compute ΔV_i using the EFD probe coordinates $\vec{l}_i$ appropriately transformed into the IGRF reference frame (the same of $\vec{v} \times \vec{B}$); once the position of the electronics box will be fixed, correct computations will be made. In such latter case, the following term will have to be added to Eq.9:

$$\Delta V = \left(\vec{v} \times \vec{B}\right) \cdot \vec{l}_{box} \tag{10}$$

TABLE 2. Coordinates of EFD probes w.r.t. the satellite-rocket docking surface. X is oriented along the satellite flight direction, Z pointing towards the Earth center and Y completes the right hand coordinates system.

	X (mm)	Y (mm)	Z (mm)
Boom A	35	-3881.2	625
Boom B	-2866	49.4	-4020.6
Boom C	4811.8	525	-3646
Boom D	1433.1	4306	3111.1

where $\vec{l}_{box}$ will be the coordinates of the electronics box with respect to the centre of satellite-rocket docking surface (also expressed in the IGRF reference frame).

All the above taken into account, the voltages of the four probes are computed and shown in Fig. 8.

VII. CONCLUSIONS

We studied the floating potential V_f and plasma sheath contact resistance R_{pl} of the EFD experiment, computed using plasma density and electron temperature determined with the IRI model along typical orbits of the CSES spacecraft mission.

The $\vec{v} \times \vec{B}$ field has been evaluated using the IGRF model to evaluate the corrective factors to apply to the probe potential measurements.

Values of V_f and R_{pl} have been computed for different values of injected bias I_b current (0, 1, 5, and 10 μA) in order to evaluate the current source setting that minimizes the plasma coupling resistance.

The threshold value of I_b, that produce a R_{pl} of the order of 10^4 Ω (considered a sufficiently low value to neglect the voltage divider attenuation at EFD amplifier input), has been identified at $\geq$ 5μA. At high frequency, the actual value of the contact impedance is further reduced by the presence of the plasma sheath capacitance C_{pl}, producing a better AC response of the EFD.

Such a condition also satisfies the requirement of having a floating potential V_f as close as possible to V_{pl}, thus improving the accuracy of the electric field measurement. Moreover, we have shown that, in the regions where the floating potential becomes positive, the R_{pl} obtained for $I_b = 5\mu$A and $I_b = 10\mu$A tend to superimpose to each other, indicating that the contact resistance becomes independent from the probe potential. As a consequence, the response of the EFD experiment, operating with the plasma parameters considered in our study, could be optimized by setting the current generator at a constant value between 5 and 10 μA for the entire orbit. Note however that exceptional plasma density minima (not modelled by IRI) could modify, for some orbits, the conclusions stated above on the I_b current source setting, requiring some re-adjustment along the orbit.

Furthermore, we have demonstrated that, a variation of the photoelectron current in the range 0 – 0.23 μA (corresponding to current densities J_{ph} between 0 and 80 μA/m^2) does not affect significantly the values of V_f and R_{pl}. This is consistent with the fact that in the ionospheric Low Earth Orbits (LEO), the relatively high density of plasma produces a negligible photoelectron contribution in the total probe current collection. Even this conclusion should be reconsidered in case of exceptional plasma density minima experienced along the orbit.

Finally, we have to point out that all our considerations are valid if we assume an approximate similarity of the plasma environment during the ongoing cycle n. 24 to what observed during the corresponding phase of the past solar cycle n. 23.

ACKNOWLEDGEMENTS

The authors would like to thank the P.I. of the EFD experiment Prof. G. Picozza (Tor Vergata Rome University). They also want to thank Dr. P. Ubertini (Director of INAF/IAPS) for making available the laboratory facility and the INAF Plasma Chamber which are currently used to experimentally verify these results.

REFERENCES

[1] J. J. Berthelier *et al.*, "ICE, the electric field experiment on DEMETER," *Planetary Space Sci.*, vol. 54, no. 5, pp. 456–471, 2006.
[2] C. Fidani, R. Battiston, W. J. Burger, and L. Conti, "A study of NOAA particle flux sensitivity to solar activity and strategies to search for correlations among satellite data and earthquake phenomena," *Int. J. Remote Sens.*, vol. 33, no. 15, pp. 4796–4814, 2012, doi: 10.1080/01431161.2011.638337.
[3] M. Parrot *et al.*, "High-frequency seismo-electromagnetic effects," *Phys. Earth Planetary Interiors*, vol. 77, pp. 65–83, Apr. 1993.
[4] X. Zhu. (2011). CSES—Satellite system introduction. DFH Satellite Co., Ltd. [Online]. Available: http://www.iaps.inaf.it/cses/Documenti/cses_satellite_system_introduction.pdf
[5] Y. Miyake, C. M. Cully, H. Usui, and H. Nakashima, "Plasma particle simulations of wake formation behind a spacecraft with thin wire booms," *J. Geophys. Res. Space Phys.*, vol. 118, pp. 5681–5694, Sep. 2013, doi: 10.1002/jgra.50543.
[6] *IRI Data From*. [Online]. Available: http://omniweb.gsfc.nasa.gov/vitmo/iri_vitmo.html
[7] R. L. Boyd, "Langmuir probes on spacecraft," in *Plasma Diagnostics*, W. Lochte-Holtgreven, Ed. Amsterdam, The Netherlands: North Holland, 1968.
[8] D. Badoni *et al.*, "An electric field detector for high-performance measurements of the electric field in the ionosphere," in *Proc. 34th Int. Cosmic Ray Conf. (ICRC)*, The Hague, The Netherlands, Jul./Aug. 2015, p. 588.
[9] G. Medicus, "Theory of electron collection of spherical probes," *J. Appl. Phys.*, vol. 32, no. 12, pp. 2512–2520, 1961.
[10] L. Schott, "Electrical probes," *Plasma Diagnostics*, W. Lochte-Holtgreven, Ed. Amsterdam, The Netherlands: North Holland, 1968.
[11] A. Giraud and M. Petit, *Ionospheric Technique and Phenomena*. Dordrecht, Holland: Reidel, 1978.
[12] N. Hershkowitz, "How Langmuir probes work," in *Plasma Diagnostics: Discharge Parameters and Chemistry*, vol. 1, O. Auciello and D. L. Flamm, Eds. San Diego, CA, USA: Academic, 1989, pp. 130–131.
[13] R. J. L. Grard, "Properties of the satellite photoelectron sheath derived from photoemission laboratory measurements," *J. Geophys. Res.*, vol. 78, pp. 2885–2906, Jun. 1973.
[14] E. Winkler, "Plasma densities and satellite potentials, a study of EUV interaction with the cluster spacecraft," Diploma thesis, Swedish Inst. Space Phys., Master Sci. Program Eng. Phys., Uppsala Univ., Uppsala, Sweden, 2007.
[15] J. J. Berthelier, private communication, 2014.
[16] A. Pedersen, F. Mozer, and G. Gustafsson, "Electric field measurements in a tenuous plasma with spherical double probes," in *Measurement Techniques in Space Plasmas Fields*, R. F. Pfaff, J. E. Borovsky, and D. T. Young, Eds. Washington, DC, USA: AGU, 1998, pp. 1–12.

[17] *IGRF Data From*. [Online]. Available: http://ccmc.gsfc.nasa.gov/modelweb/models/igrf_vitmo.php
[18] X. Zhu, private communication, 2016. [Online]. Available: http://www.iaps.inaf.it/cses/Documenti/Answer_to_Question_List_2016.pdf

PIERO DIEGO was born in Oriolo, Italy, in 1969. He received the degree in physics from Rome Three University, Italy, in 2002, and the Ph.D. degree in science of the Earth from the University of Siena, Italy, in 2007.

From 2002 to 2005, he was with the Institute of Interplanetary Space Physics in Solar-Terrestrial relationship physics. Then, he was for several years in Cosmic Ray detectors research field (SVIRCO observatory). During this period, he participated in three Antarctic campaigns from 2005 to 2007 for the installation of a Neutron Monitor for the Cosmic Ray records. After this period, he was with plasma physics research field, studying solar wind perturbations in the interplanetary medium and ionospheric plasma properties as well. He is currently responsible of the INAF-IAPS Plasma Chamber that is a facility able to reproduce the ionospheric plasma at LEO orbit. For this activity, he has received, from the Italian Space Agency, the management role for testing and calibration of several CSES Chinese satellite payloads.

IGOR BERTELLO was born in Rome, in 1971. He received the Laurea degree in physics from the University of Rome La Sapienza, Roma, Italy, in 2001.

In 2002, he joined the Gifint Group, Interplanetary Space Physics Institute (IFSI), Italian National Council of Research. At IFSI, he was mainly involved in the study and implementation of neural network algorithms for now casting and forecasting of magnetic storms. After a brief period, he was with the electronic industry, then he returned to the activity of Researcher with INAF-IAPS (Italian Insitute of Astro Physics), where he is currently involved with the Ionospheric Plasma Chamber in test activities of satellites plasma payloads.

MAURIZIO CANDIDI was born in Rome, in 1943. He received the Laurea degree from the Faculty of Physics, University of Rome, in 1968.

He joined Laboratorio Plasma Spazio, CNR, the National Research Council of Italy, in 1970, and performed research on Earth magnetosphere and Interplanetary Space Physics throughout his career. He was a Visiting Scientist in several U.S. research centers, NOAA, Boulder, CO, and Johns Hopkins University, Laurel, MD, for extended periods. He was involved in the preparation and flight data analysis for several space missions, in particular, a Mission Scientist for the Thetered Satellite System Mission. He collaborated for several years with the Italian Antarctic Program, leading the Astronomy and Space Physics National Community. He was elected as a Chief Officer of the Physical Sciences Standing Scientific Group, Scientific Committee for Antarctic Research (SCAR), ICSU. He was nominated by SCAR as Liaison to SCOSTEP, the Scientific Committee for Solar TErrestrial Physics of ICSU. He served as the Director of the Interplanetary Space Physics Institute (IFSI), CNR. He has been the Research Director since 2008, still holding a position as an Associate Scientist of IAPS, Space Astrophysical and Planetology Institute, INAF, the National Astrophysical Institute of Italy.

ALESSANDRO MURA was born in Udine, Italy, in 1970. He received the degree (*summa cum laude*) in physics from the University of Rome La Sapienza, in 1998, and the Ph.D. degree in physics, in 2004.

He joined the Institute of IAPS Space Astro-Physics and Planetology Institute in 2000 as a Contractor Researcher. Since then, he was a Team Member of ASPERA-3 instrument on board ESA-MeX Mission, responsible for ASPERA-3 Data Display Unit and web-based data display, and managed the IFSI archive of ASPERA-3 data. As for scientific activity, he developed original studies in planetary (Earth, Mars, and Mercury) space physics. In 2008, he got a permanent position as a Researcher with IAPS/INAF. He is currently the Deputy-PI of JIRAM instrument on board NASA-JUNO Mission, the Co-I of ASPERA-4 instrument on board ESA-VeX Mission, and the Co-I of SERENA instrument on board ESA-BepiColombo Mission (ELENA/SERENA Core Member, responsible of ELENA instrument operations, performance, and signal simulation).

GIULIANO VANNARONI was born in Rome, Italy, in 1948. He received the Laurea (*cum laude*) degree in physics from the University of Rome La Sapienza, Rome, in 1984.

In 1985, he joined the Italian National Council of Research, Interplanetary Space Physics Institute (IFSI), Frascati, Italy, as a Staff Scientist. At IFSI, he was mainly involved in the studies on laboratory simulations of electrodynamic interactions between LEO spacecrafts and ionosphere, and relevant plasma diagnostics. He performed studies on electrodynamic tether systems for deorbiting and propulsion applications, and was the Principal Investigator of the RETE experiment flown in 1996 onboard the reflight mission Tethered Satellite System TSS-1R. In 2001, he joined the Team of Mars Surveyor Program Lander Mission (ACQUA experiment) where he was involved in studies on electromagnetic techniques and dielectric spectroscopy methods applied to the search for liquid or iced water in planetary subsurfaces. In 2007, he retired from the Interplanetary Space Physics Institute maintaining the position of Associated Scientist and was a Contract Professor of Physics and Mathematics with the Università degli Studi della Tuscia, Viterbo, Italy, for seven years. He is currently involved, as an Associated Scientist, in test activities on CSES plasma payloads using the Ionospheric Plasma Chamber, INAF-IAPS, Rome.

DAVIDE BADONI received the Laurea degree in physics from the University of Roma Tor Vergata, Roma, Italy, in 2005. He was a Professor of Electronics Physics and Applied Cybernetics with the Science Faculty, University of Roma Tor Vergata. He is in the permanent staff of the Italian Institute for Nuclear Physics and has been teaching Microelectronics at the Physics Department, University of Roma Tor Vergata since 2011. His main fields of research interest and activities include study of physical-sensor systems and modeling of sensors used in the fields of particle physics and astroparticle physics, modeling and implementation of neural networks with dynamic learning, VLSI design of submicron microelectronics of full-custom analog and mixed signal electronic systems. He has co-authored 23 internationally refereed publications and has co-authored several conference proceedings and presentation.